Biosensors and Bioelectronics 130 (2019) 81–87

Contents lists available at ScienceDirect

Biosensors and Bioelectronics

journal homepage: www.elsevier.com/locate/bios

An ultrasensitive electrochemical biosensor for detection of microRNA-21 based on redox reaction of ascorbic acid/iodine and duplex-specific nuclease assisted target recycling

Jin Wang[a,b], Jian Lu[b], Shuaibing Dong[a], Nuanfei Zhu[a], Eric Gyimah[a], Kun Wang[c], Yong Li[d], Zhen Zhang[a,*]

[a] School of the Environment and Safety Engineering, Jiangsu University, Zhenjiang 212013, China
[b] Institute of Life Sciences, Jiangsu University, Zhenjiang 212013, China
[c] The School of Chemistry and Chemical Engineering, Jiangsu University, Zhenjiang 212013, China
[d] School of Environmental Science and Engineering, Suzhou University of Science and Technology, Suzhou, China, 215009

ARTICLE INFO

Keywords:
MicroRNA detection
Signal amplification
Duplex-specific nuclease
Target recycling
Electrochemical biosensor

ABSTRACT

A novel electrochemical biosensor was developed based on multiwall carbon nanotubes/graphene oxide nanoribbons (MWCNTs/GONRs) for sensitive analysis of microRNA-21. Signal-amplified strategy was achieved by duplex-specific nuclease assisted target recycling and alkaline phosphatase-induced redox reactions. At the fabrication process of the sensor, ssDNA capture probes were immobilized on the surface of the MWCNTs@GONRs/AuNPs modified electrode through the Au-S bond, and the streptavidin-conjugated alkaline phosphatase (SA-ALP) was attached to the end of the probe. In the absence of miRNA-21, SA-ALP catalysed the conversion of ascorbic acid 2-phosphate (AAP) into ascorbic acid (AA), triggered a redox reaction under iodine, producing a marked electrochemical response. When miRNA-21 was hybridized to the capture probe, the duplex would be cleaved by the duplex-specific nuclease (DSN), causing the electrochemical signals being significantly decreased as a result of SA-ALP detached from the electrode surface. Under the optimized conditions, our biosensor showed satisfactory sensitivity (detection limit, 0.034 fM), excellent selectivity and good accuracy (recoveries, 77.4–120.2%; RSD, 5.2–7.3%) after systematic evaluations. The proposed approach was applied to detect miRNA-21 from human serum samples, which indicated that it was reliable and could be widely used as an effective tool for rapid detection of the target in serums.

1. Introduction

MicroRNAs (miRNAs) are classes of non-coding small RNAs (19–23 nts) that regulate the expression of multiple genes by degrading or blocking mRNAs translation (Blenkiron et al., 2007; Carrington and Ambros, 2003), which are closely related to the cell proliferation and differentiation, development and progression of cancer (Gaur et al., 2007; Lu et al., 2005; Ventura and Jacks, 2009). Since miRNAs can be stably stored in serum (Sarah Grasedieck et al., 2013; Weber et al., 2010), they could be used as an important biomarker for early diagnosis of the corresponding diseases. Therefore, development of a suitable analytical method for rapid detection of miRNAs is needed.

Currently available methods for the determination of miRNA were reported like Northern blotting, real-time quantitative PCR (qPCR) and DNA microarrays (Chen et al., 2011; Yang et al., 2018, 2017). Although these approaches displayed some advantages in biological research fields, they suffered from complicated operation, low sensitivity and high cost. In contrast, the electrochemical biosensor was regarded as a sensitive analytical method to quickly measure signals using simple devices (Lu et al., 2018; Miao et al., 2018), which is suitable for detection of miRNA from various samples. Furthermore, by means of unique properties of nanoparticles, the sensitivity of the electrochemical biosensor can be significantly improved.

Owing to the excellent flexibility, ductility and electrical conductivity, multiwall carbon nanotubes/graphene oxide nanoribbons (MWCNTs/GONRs) have been widely used in the field of electrochemical analysis since the past years (Li et al., 2010; Lv et al., 2014). Actually, we also introduced MWCNTs/GONRs into the electrochemical immunoassays where the specific surface area of the electrode was remarkably increased to load more antibodies, contributing to good

* Corresponding author.
E-mail address: zhangzhen@ujs.edu.cn (Z. Zhang).

https://doi.org/10.1016/j.bios.2019.01.031
Received 14 November 2018; Received in revised form 17 December 2018; Accepted 8 January 2019
Available online 21 January 2019
0956-5663/

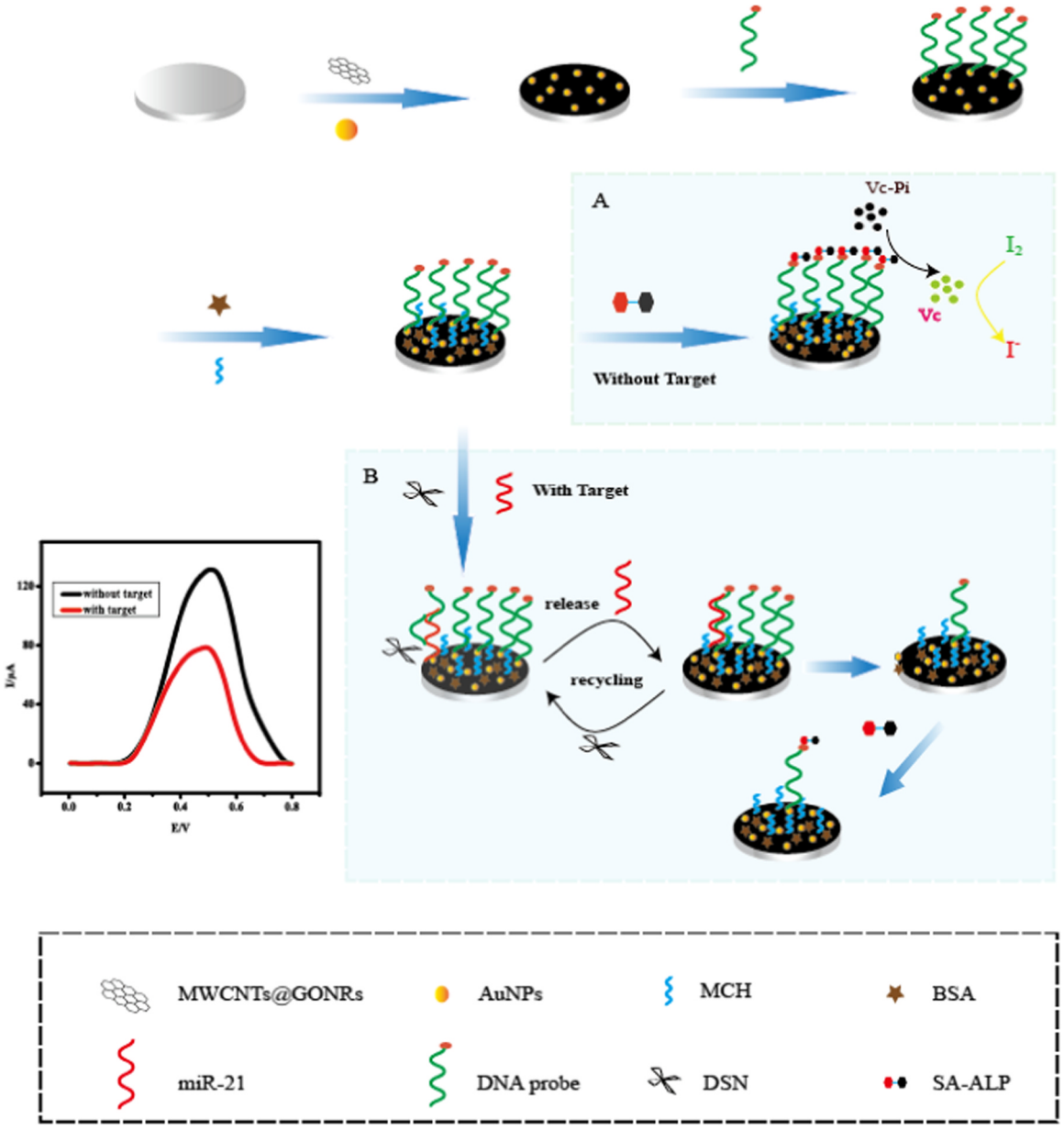

Scheme 1. Schematic illustration of the electrochemical biosensor for the detection of miRNA-21.

sensitivity (Liang et al., 2017; Lu et al., 2018). Besides, duplex-specific nuclease (DSN) is a novel stable double-strand specific nuclease isolated from the hepatopancreas of Kamchatka crab, which possesses abundant cleavage preference for DNA in DNA-RNA hybrids, but not for single-stranded DNA (Shagin et al., 2002). Moreover, DSN has a good discrimination between perfectly matched and non-fully matched duplexes, and exhibit a good selectivity for miRNAs (Shuai et al., 2017; Zhang et al., 2016).

In this work, an ultrasensitive electrochemical biosensor was designed for the rapid determination of miRNA-21. MWCNTs/GONRs was used to immobilize massive cDNA probes for improving sensitivity, and signal amplification was implement through DSN-assisted target recycling. After evaluation of its selectivity, performance, accuracy and precision, the established method was applied for real samples measurement.

2. Experimental

2.1. Reagent and materials

Multi-walled carbon nanotube (MWCNT) was obtained from Aladdin-Regent, Inc. 6-mercap-tohexanol (MCH) was provided by Meryer Chemical technology Co, Ltd. (Shanghai), AuNPs were bought from Shanghai Jieyi Co., Ltd.(Shanghai). Duplex-specific nuclease was supplied by Evrogen Joint Stock Company (Moscow, Russia). MiRNA and DNA sequences were synthesized by Shanghai Sangon Biological Engineering Technology Co. Ltd. (Shanghai, China) and their sequences can be seen in Table S1.

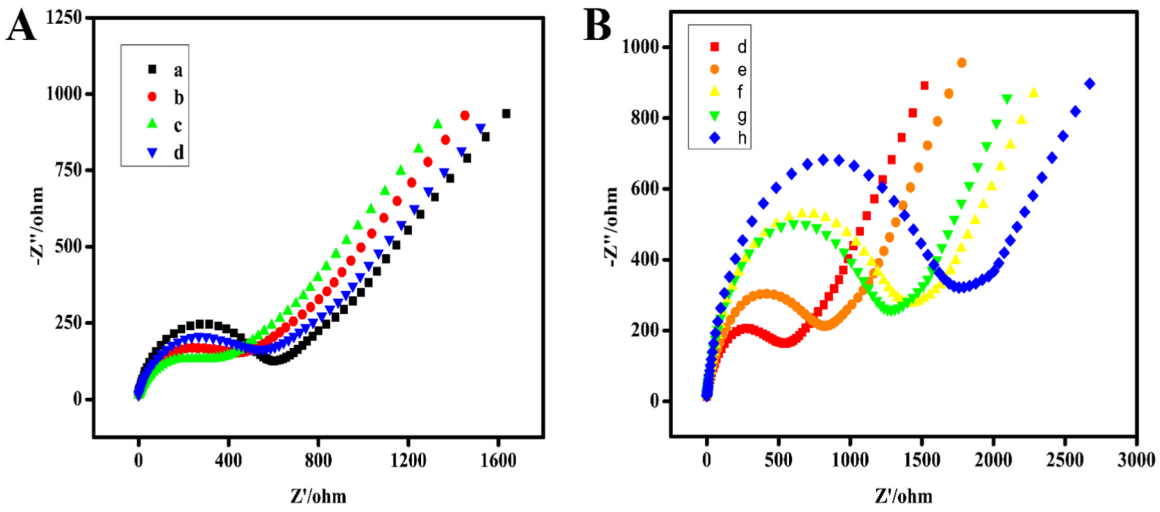

Fig. 1. A and B The impedimetric characteristics of the developed biosensor. (**a**) Bare GCE; (**b**) MWCNTs@GONRs/GCE; (**c**) AuNPs/MWCNTs@GONRs/GCE; (**d**) Capture DNA/AuNPs/MWCNTs@GONRs/GCE; (**e**) MCH/Capture DNA/AuNPs/MWCNTs@GONRs/GCE; (**f**) BSA/MCH/Capture DNA/AuNPs/MWCNTs@GONRs/GCE; (g) BSA/MCH/Capture DNA/AuNPs/MWCNTs@GONRs/GCE after reacted with miRNA/DSN; (h) SA-ALP/BSA/MCH/Capture DNA/AuNPs/MWCNTs@GONRs/GCE.

2.2. Apparatus

Electrochemical measurements were performed on CHI660E electrochemical workstation (Shanghai Chen Hua Instrument Co., China) with a three-electrode system composed of a saturated calomel electrode (SCE) as reference electrode, a platinum wire as an auxiliary electrode, and a 3 mm diameter glassy carbon electrode (GCE) as working electrode. Transmission electron microscopy (TEM) images were obtained using a JEM 2100 transmission electron microscope (TEM, JEOL, Tokyo, Japan).

2.3. Preparation of the MWCNTs@GONRs

MWCNTs@GONRs were prepared according to the previously reported work (Lu et al., 2018). In short, 120 mg MWCNTs and 40 mL H_3PO_4/H_2SO_4 (1:9) were added to a round-bottomed flask and stir well, after addition of 600 mg $KMnO_4$, the mixture was kept stirring for 2 h at 65 °C. Then, 400 mL ice water containing 0.75% H_2O_2 were added into the solution. Finally, the MWCNTs@GONRs was generated through steps of purification and stored at 4 °C for until needed for analysis.

2.4. Preparation of the modified GCE and electrochemical measurements

The bare glassy carbon electrode (GCE, φ = 3.0 mm) was polished with 1.0, 0.3, and 0.05 μm Al_2O_3 slurries on the chamois leather. After ultrasonic cleaning with ethanol solution, the GCE was washed again with ultrapure water and dried at room temperature.

Subsequently, 6 μL MWCNTs@GONRs (0.5 mg/mL) was applied on the cleaned electrode surface. Then, 6 μL AuNPs was dropped onto the electrode to assemble DNA capture probe. Afterwards, 6 μL DNA capture solution (cDNA, 1 nM) was applied onto AuNPs/MWCNTs@GONRs/GCE and allowed to react at 37 °C overnight. After being washed with ultrapure water, 6 μL BSA (1%) and 1 nM MCH were dropped on the electrode and kept for 0.5 h to block non-specific binding sites. Through the washing step, 4.5 μL miRNA-21 (1 nM) and 1.5 μL DSN (0.01 U) were mixed under the at 65 °C for 1 h. After the mixture has been washed, 6 μL SA-ALP (0.1 mg/mL) was added on the surface of the electrode and maintained for 40 min at 37 °C. Finally, the electrode was submerged in a 10 mL Tris-HCl buffer solution (10 nM, pH 8.0) with 5 mM AAP and 1 mM $MgCl_2$ for 30 min. After further washing the electrode with ultrapure water, the electrode was used for electrochemical measurements.

The electrochemical impedance spctroscopy (EIS) measurements were conducted in a 0.01 mol/L PBS (pH 7.4) solution containing 5.0 mmol/L Fe $(CN)_6^{3-/4-}$ at a frequency range of 10^{-1}–10^4 Hz. The differential pulse voltammetry (DPV) experiments were implemented in Tris buffer solution containing 25 mM I_2 and 50 mM KI with the following pulse conditions: 0.2 s (period), 50 mV (amplitude) and of 50 ms (width).

3. Results and discussion

3.1. Detection strategy of the biosensor

The principle of our biosensor for sensitive analysis of miRNA was illustrated as Scheme 1. In this assay, the cDNA probe is immobilized on the AuNPs/MWCNTs@GONRs/GCE using the Au-S bond, which was connected to SA-ALP through streptavidin-biotin interaction, leading to the catalytic dephosphorylation of AAP to AA, which could reduce I_2 into I^- (Meissam and Hamed, 2011). According to the equation ($I_2 + I^- \rightleftharpoons I_3^-; I_3^- + AA \rightarrow 3I^- + DAA + 2H^+$), the added KI in the system could improve the solubility of I_2 in solution. In addition, this redox reaction can bring about electron transfer and generate significant electrochemical signals. Once the miRNA is hybridized to the capture probe, the DSN enzyme will cleave the cDNA, leaving the SA-ALP away from the electrode surface. At the same time, the intact miRNA strand is released and continues to participate the recycling in the sample. During incubation of the double strand with the DSN enzyme, a miRNA molecule will bind to massive capture probes and cause DNA strand broken, resulting in a significant signal reduction, being conducive to obtain low detection limit. At the process, when the concentration of miRNA is gradually increased, correspondingly, the oxidation current of the system will decrease step by step.

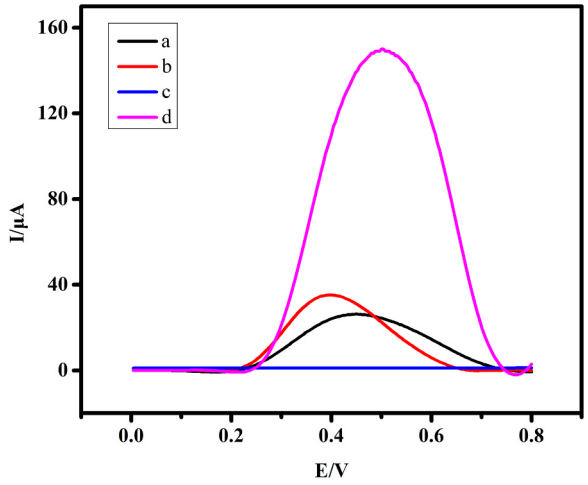

Fig. 2. DPVs of BSA/MCH/Capture DNA/AuNPs/MWCNTs@GONRs/GCE in different solutions: (a) SA-ALP/I_2; (b) AAP/I_2; (c) SA-ALP/AAP; (d) SA-ALP/AAP/I_2.

3.2. Electrochemical characterization

EIS is one of the common methods used to explore the modification of the electrode surface (Yang et al., 2017). Fig. 1**A** and **B** show the Nyquist diagrams of gradual modification processes measured in PBS buffer (pH 7) containing 5 mmol/L Fe $(CN)_6^{3-/4-}$ and 0.1 mol/L KCl, in which the Nyquist plot consists of a linear part (corresponding to a diffusion-limited process) and a semi-circular part (representing an electron transfer-limited process, and the diameter of the semicircle is equal to electron transfer resistance, Ret) (Peng et al., 2016; Zhang et al., 2018). In comparison with the bare GCE (**curve a**, 606 Ω), **curve b** indicated that Ret was significantly reduced after MWCNTs@GONRs was decorated onto the electrode owing to its good electro-conductivity. The similar phenomenon also was observed after modifying AuNPs on the electrode surface (**curve c**). Meanwhile, distinct increases of Ret value was generated when the electrodes were respectively functionalized by the capture probe, MCH and BSA, which was because these substances blocked the path of electron transport (**curve d**, **e** and **f**). We also found that when SA-ALP is added to the surface of electrode, Ret value was greatly enhanced **(curve h)**, attributed to the enlarged distance between the Fe $(CN)_6^{3-/4-}$ redox pair and the electrode surface. However, due to the reason that DSN cleaved cDNA strand, Ret was significantly declined after miRNA/DSN completely incubated (displayed in **curve g**). The above EIS results showed that we have successfully modified the electrodes and this proposed method can be used for the targets detection.

3.3. Feasibility of analytical methods

According to our design, AAP would be transformed to AA under the catalysis by SA-ALP, triggered the reduction reaction of I_2 to I^-, resulting in the corresponding electrochemical signals. Therefore, this step is the most important factor in the fabrication of the biosensor. To assess the key step, the DPV responses under different situations were adopted. As displayed in Fig. 2, only weak oxidation currents can be detected **(curve a** and **b)** without AAP or SA-ALP. In addition, no redox reaction was observed in the absence of I_2 **(curve c)**. In contrast, when AAP, SA-ALP and I_2 are simultaneously present in the solution, significant peak currents was obtained, indicating that the reaction system was successfully constructed **(curve d)**.

3.4. Optimization of the biosensor

Given that several parameters can affect the performance of the biosensor (including the concentrations of DSN, SA-ALP and I_2, incubation time), they were estimated in details using the DPV as a standard.

The working temperature of DSN was carried out at 65 °C, which was in accordance with the previous protocol (Liu et al., 2014), Under this condition, the concentration and reaction time of DSN were tested. Seen from Fig. 3**A**, DPV signal originally decreased with increasing concentration of DSN, and in turn become stable at 0.01U. Accordingly, 0.01U was selected as the optimized concentration for DSN. Meanwhile, a similar trend was observed in Fig. 3**B**, demonstrating that the reaction could be almost accomplished within 60 min.

The most suitable concentration of SA-ALP was investigated through its serial concentrations (0.02, 0.04, 0.06, 0.08, 0.10, 0.12, 0.16 mg/mL), Displayed by Fig. 3**C**, the maximum DPV values was obtained under the concentration of 0.1 mg/mL, which was considered as the optimized concentration for SA-ALP. At the same time, our results also revealed that 40 min was the optimal time for the reaction (Fig. 3**D**). Besides, after detailed investigation, the maximum intensity of the DPV signal was generated when the concentration of I_2 reached 25 mM (Fig. 3**E**), implying that this is the optimal concentration for I_2 in this system.

Under above mentioned conditions, a standard curve was established (Fig. 4**B**) using Origin software (version 8.0) according to a range of concentrations of miRNA measurements (Fig. 4**A**), and the detection limit of the method was 0.034 fM (S/N = 3) with the correlation coefficient R = 0.992 using the linear calibration equation ($\Delta I = 123.8 + 7.68 \log(c/M)$), ($\Delta I = I_0 - I$, I and I_0 represent peak current when miRNA exists or not, respectively). Compared to the reported approaches for miRNA determination (shown in Table S3), our biosensor demonstrated obvious merits in performance.

3.5. Selectivity

To verify the selectivity of the established method, different miRNA sequences were used for its evaluation. Fig. 5 indicates that the complementary sequence had the highest ΔI. By comparison, the results of the experiment show that other miRNAs cannot trigger the expected reactions, thus negligible ΔI are measured. And the above results indicate an excellent selectivity of this biosensor.

3.6. Verification of accuracy and sample analysis

The accuracy and precision of our method were evaluated using a spike-recovery analysis from PBS solution (containing 1% human serum) fortified with a variety of miRNA concentrations. Table S2 indicated that the miRNA recoveries were in the range of 77.4–120.2% with the RSD from 5.2% to 7.3%, implying that the method is reliable and could be used for real sample analysis.

The established method was applied to detect miRNA from various blood samples collected from 5 healthy donors and 5 breast cancer patients (confirmed by pathological examinations), which were provided by Affiliated Hospital of Jiangsu University. All blood samples were treated by centrifugation at 3000 r/min for 1 min to obtain serums. As shown in Fig. S4 and S5, serum samples from cancer patients generated lower DPV signals than that from healthy donors, indicating up-regulation of miRNA-21 expression in serums of breast cancer, consistent with the results reported in literature (Asaga et al., 2011; Wang et al., 2010). We also compared the biosensor with commercial qRT-PCR kit, as shown in Table S4, the results obtained with the biosensor were in good agreement with those obtained by qPCR,

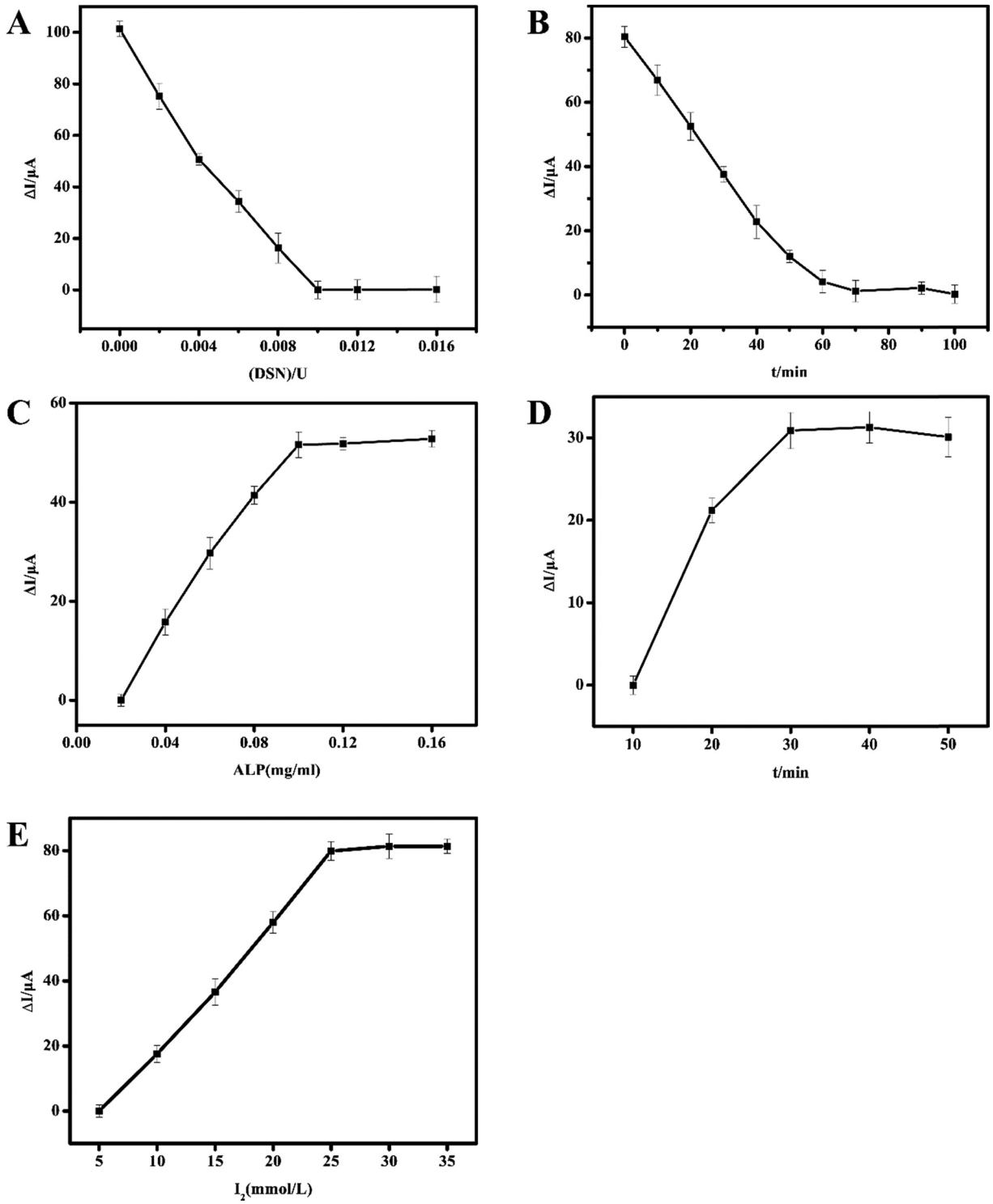

Fig. 3. Effects of DSN concentration on DPV response (A); Effects of reaction time of DSN on DPV response (B); Effects of ALP concentration on DPV response (C); Effects of reaction time of ALP on DPV response (D); Effects of I_2 concentration on DPV response (E).

confirming the practical value of developed biosensor.

4. Conclusions

In summary, we have developed a sensitive electrochemical sensor for rapid detection of miRNA-21. The detection system is based on the specific recognition of miRNA-DNA duplexes by DSN enzymes coupling with the excellent electrochemical performance of MWCNTs@GONRs to achieve signal amplification. Through a series of verification, the established method demonstrated excellent selectivity, good accuracy and satisfactory sensitivity (LOD, 0.034 fM), which can be widely applied for early diagnosis of cancer.

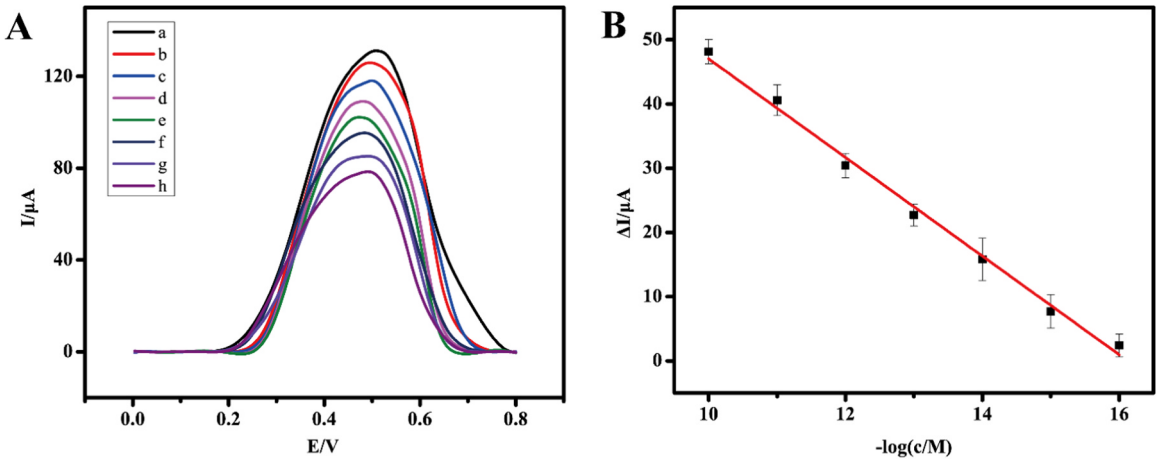

Fig. 4. DPV curves responding to different miRNA concentrations (from a to h): 0, 1.0×10^{-16}, 1.0×10^{-15}, 1.0×10^{-14}, 1.0×10^{-13}, 1.0×10^{-12}, 1.0×10^{-11}, 1.0×10^{-10} M, respectively (A); The linear relationship between the current variation ΔI and the negatively logarithm of the miRNA concentration (B).

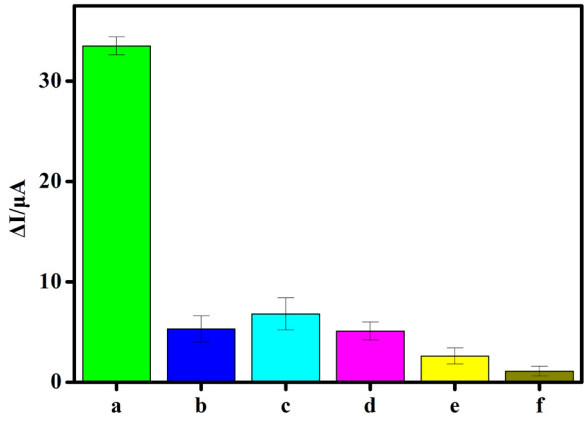

Fig. 5. The selectivity of the sensor hybridized to different miRNA sequences: (a) miR-21; (b) single-base mismatched miR-21a; (c) single-base mismatched miR-21b; (d) single-base mismatched miR-21c; (e) three-base mismatched miR-21; (f) noncomplementary miR-21.

CRediT authorship contribution statement

Jin Wang: Conceptualization, Data curation, Methodology, Writing - original draft. **Jian Lu:** Conceptualization. **Shuaibing Dong:** Data curation, Methodology. **Nuanfei Zhu:** Data curation, Methodology. **Eric Gyimah:** Writing - review & editing. **Kun Wang:** Visualization. **Yong Li:** Visualization. **Zhen Zhang:** Writing - review & editing.

Acknowledgement

The present work was supported by the National Natural Science Foundation of China (Grants 21577051, 21876067) and the Jiangsu Collaborative Innovation Center for Technology and Water Treatment.

Declaration of interests

None.

Appendix A. Supporting information

Supplementary data associated with this article can be found in the online version at doi:10.1016/j.bios.2019.01.031.

References

Asaga, S., Kuo, C., Nguyen, T., Terpenning, M., Giuliano, A.E., Hoon, D.S., 2011. Direct serum assay for microRNA-21 concentrations in early and advanced breast cancer. Clin. Chem. 57 (1), 84–91.

Blenkiron, C., Goldstein, L.D., Thorne, N.P., Spiteri, I., Chin, S.-F., Dunning, M.J., Barbosa-Morais, N.L., Teschendorff, A.E., Green, A.R., Ellis, I.O., Tavaré, S., Caldas, C., Miska, E.A., 2007. MicroRNA expression profiling of human breast cancer identifies new markers of tumor subtype. Genome Biol. 8 (10) (R214-R214).

Carrington, J.C., Ambros, V., 2003. Role of microRNAs in plant and animal development. Science 301 (5631), 336.

Chen, C., Tan, R., Wong, L., Fekete, R., Halsey, J., 2011. Quantitation of microRNAs by real-time RT-qPCR. In: Park, D.J. (Ed.), PCR Protocols. Humana Press, Totowa, NJ, pp. 113–134.

Gaur, A., Jewell, D.A., Liang, Y., Ridzon, D., Moore, J.H., Chen, C., Ambros, V.R., Israel, M.A., 2007. Characterization of microRNA expression levels and their biological correlates in human cancer cell lines. Cancer Res. 67 (6), 2456–2468.

Li, C., Li, Z., Zhu, H., Wang, K., Wei, J., Li, X., Sun, P., Zhang, H., Wu, D., 2010. Graphene nano-"patches" on a carbon nanotube network for highly transparent/conductive thin film applications. J. Phys. Chem. C. 114 (33), 14008–14012.

Liang, Y.-R., Zhang, Z.-M., Liu, Z.-J., Wang, K., Wu, X.-Y., Zeng, K., Meng, H., Zhang, Z., 2017. A highly sensitive signal-amplified gold nanoparticle-based electrochemical immunosensor for dibutyl phthalate detection. Biosens. Bioelectron. 91, 199–202.

Liu, L., Xia, N., Liu, H., Kang, X., Liu, X., Xue, C., He, X., 2014. Highly sensitive and label-free electrochemical detection of microRNAs based on triple signal amplification of multifunctional gold nanoparticles, enzymes and redox-cycling reaction. Biosens. Bioelectron. 53, 399–405.

Lu, J., Getz, G., Miska, E.A., Alvarez-Saavedra, E., Lamb, J., Peck, D., Sweet-Cordero, A., Ebert, B.L., Mak, R.H., Ferrando, A.A., Downing, J.R., Jacks, T., Horvitz, H.R., Golub, T.R., 2005. MicroRNA expression profiles classify human cancers. Nature 435 (7043), 834–838.

Lu, J., Tang, M., Liu, Y., Wang, J., Wu, Z., 2018. Comparative proteomics of chromium-transformed Beas-2B cells by 2D-DIGE and MALDI-TOF/TOF MS. Biol. Trace Elem. Res. 185 (1), 78–88.

Lv, R., Cruz-Silva, E., Terrones, M., 2014. Building complex hybrid carbon architectures by covalent interconnections: graphene–nanotube hybrids and more. ACS Nano 8 (5), 4061–4069.

Meissam, M., Hamed, 2011. Determination of ascorbic acid by a modified multiwall carbon nanotube paste electrode using cetrimonium iodide/iodine. Turk. J. Chem. 36 (2012), 645–658.

Miao, P., Zhang, T., Xu, J., Tang, Y., 2018. Electrochemical detection of miRNA combining T7 exonuclease-assisted cascade signal amplification and DNA-templated copper nanoparticles. Anal. Chem. 90 (18), 11154–11160.

Peng, K., Zhao, H., Xie, P., Hu, S., Yuan, Y., Yuan, R., Wu, X., 2016. Impedimetric aptasensor for nuclear factor kappa B with peroxidase-like mimic coupled DNA nanoladders as enhancer. Biosens. Bioelectron. 81, 1–7.

Sarah Grasedieck, A.S., Langer, Christian, Buske, Christian, D¨ohner, Hartmut, Mertens, Daniel, Kuchenbauer, Florian, 2013. Circulating microRNAs in hematological diseases: principles, challenges, and perspectives. Blood 121, 4977.

Shagin, D.A., Rebrikov, D.V., Kozhemyako, V.B., Altshuler, I.M., Shcheglov, A.S., Zhulidov, P.A., Bogdanova, E.A., Staroverov, D.B., Rasskazov, V.A., Lukyanov, S., 2002. A novel method for SNP detection using a new duplex-specific nuclease from crab hepatopancreas. Genome Res. 12 (12), 1935–1942.

Shuai, H.-L., Huang, K.-J., Chen, Y.-X., Fang, L.-X., Jia, M.-P., 2017. Au nanoparticles/hollow molybdenum disulfide microcubes based biosensor for microRNA-21 detection coupled with duplex-specific nuclease and enzyme signal amplification. Biosens. Bioelectron. 89, 989–997.

Ventura, A., Jacks, T., 2009. miRNAs and cancer: a little RNA goes a long way. Cell 136 (4), 586–591.

Wang, F., Zheng, Z., Guo, J., Ding, X., 2010. Correlation and quantitation of microRNA aberrant expression in tissues and sera from patients with breast tumor. Gynecol. Oncol. 119 (3), 586–593.
Weber, J.A., Baxter, D.H., Zhang, S., Huang, D.Y., How Huang, K., Jen Lee, M., Galas, D.J., Wang, K., 2010. The microRNA spectrum in 12 body fluids. Clin. Chem. 56 (11), 1733–1741.
Yang, D., Cheng, W., Chen, X., Tang, Y., Miao, P., 2018. Ultrasensitive electrochemical detection of miRNA based on DNA strand displacement polymerization and Ca2+-dependent DNAzyme cleavage. Analyst.
Yang, Z., Lan, Q., Li, J., Wu, J., Tang, Y., Hu, X., 2017. Efficient streptavidin-functionalized nitrogen-doped graphene for the development of highly sensitive electrochemical immunosensor. Biosens. Bioelectron. 89, 312–318.
Zhang, J., Wu, D.-Z., Cai, S.-X., Chen, M., Xia, Y.-K., Wu, F., Chen, J.-H., 2016. An immobilization-free electrochemical impedance biosensor based on duplex-specific nuclease assisted target recycling for amplified detection of microRNA. Biosens. Bioelectron. 75, 452–457.
Zhang, L., Xiao, X., Xu, Y., Chen, D., Chen, J., Ma, Y., Dai, Z., Zou, X., 2018. Electrochemical assay for continuous monitoring of dynamic DNA methylation process. Biosens. Bioelectron. 100, 184–191.